Available online at www.sciencedirect.com

ScienceDirect

Ceramics International 40 (2014) 4149–4154

CERAMICS INTERNATIONAL

www.elsevier.com/locate/ceramint

Heat treatment of 6H-SiC under different gaseous environments

Woo Jin Lee[a,*], Chaoen Li[a], Nick Burke[a], Jim Patel[a], Merrill Wilson[b], Karl Gerdes[c]

[a]CSIRO Earth Science and Resource Engineering, 71 Normanby Rd., Clayton North, Victoria 3169, Australia
[b]Ceramatec Inc., 2425 South, 900 West, Salt Lake City, UT 84119, USA
[c]Process Engineering Division, Chevron Energy Technology Company, 100 Chevron Way, Richmond, CA 94802, USA

Received 18 July 2013; accepted 16 August 2013
Available online 26 August 2013

Abstract

Silicon carbide is a useful material for the reactors in chemical processes. In recent years, microreactors have gained significant attentions due to the high demand for process miniaturization. As heat and mass-transfer are highly improved inside the gas flow channels in microreactors, any change on the surface of inner channels under heating becomes critical to the performance of microreactors. To investigate the surface changes of silicon carbide during the heat treatment, 6H-SiC coupons were processed in five different gases—Ar, N_2, air, 0.9% O_2 in Ar and 50% H_2O in air—that are commonly encountered in high temperature chemical processes. While the formation of oxide film was found to be dependent on the partial pressure of oxidizing gas, surface decomposition was found from the treatment in nitrogen environment. Characterization of the SiC surface by Raman spectroscopy and SEM–EDX revealed that a graphitic layer has formed at the oxide film/SiC interface. Crystallinity of graphitic layer at the interface seemed to be dependent on the partial pressure of oxidizing gas, which was revealed by the relationship between G peak position and $R(I_D/I_G)$. The intensity ratio of FTO(0)/FTO(2/6) bands showed that stacking faults on the surface of SiC coupons were reduced after heat treatment.

Keywords: B. Interfaces; D. Silicon carbides; Heat treatment; Raman spectroscopy

1. Introduction

Silicon carbide (SiC) possesses highly desirable properties, such as superior thermal conductivity and mechanical strength, and consequently SiC has received a great deal of attention as a high performance material for a range of applications [1,2]. These properties, combined with its excellent chemical inertness, make SiC suitable for the component of reactors, which are often exposed to severe conditions in gas-phase chemical processes. Several different types of SiC reactors have been described for such applications in literature [3–5]. In recent years, due to a high demand for process miniaturization, the use of microstructured reactors for chemical processes has gained considerable attention [6–8]. Typically, inside the narrow channels of microstructured reactors, the heat and mass transfers are largely enhanced compared to conventional reactors [8]. Therefore, during the operation of this type of small-scale reactors, structural changes on the surface of inner walls, even at a microscopic scale, may critically affect the performance of the reactor. Our recent study showed that microstructures have formed on SiC surfaces after being exposed to methane oxyreforming conditions [9]. Growth of carbon-related microstructure on the surface of reactors will affect significantly heat and mass transfer, in particular, for a narrow flow path in micro-scaled reactors. This led us to investigate the fundamental processes that occurred on the SiC surface during the heat treatment under different gaseous environments. To clearly differentiate the effect of gases used for heat treatment on the behavior of SiC surface, we have selected the conditions that are typically encountered in the gas processing applications such as high temperature argon, nitrogen and oxygen-containing environments.

Hexagonal 6H-SiC is often used for making SiC-based devices. In this study, we employed polycrystalline 6H-SiC coupons to investigate the changes on SiC surfaces upon heat treatment with different gases at high temperatures. In other words, the inner surface of SiC-based microscaled reactors can be simulated by the surface of coupons used in this study. After heat treatment, Raman spectroscopy, which is a powerful

*Corresponding author. Tel.: +61 39 545 8375; fax: +61 39 545 8380.
E-mail address: WooJin.Lee@csiro.au (W.J. Lee).

0272-8842/$ - see front matter
http://dx.doi.org/10.1016/j.ceramint.2013.08.071

and non-destructive technique for exploring the structural changes on SiC surfaces [10–12], was employed to investigate the surface of SiC. The results from Raman spectra were present with the findings from scanning electron microscopy (SEM) combined with energy dispersive X-ray spectroscopy (EDX) in this study.

2. Experimental

To perform the heat treatment experiments, 12 pressureless-sintered 6H-SiC coupons of 50 (L) × 4.75 (W) × 0.72 (D) mm^3 (Ceramatec Co., USA) were stacked in a vertical SiC reactor with an inner diameter of 6 mm (Hexoloy SA, Saint-Gobain Ceramics, USA). For the sake of convenience, in this paper we describe the position inside the reactor according to the coupon number, with coupon-1 being that located at the top of the reactor (see Fig. 4c). The reactor was heated in an electric furnace to 1400 °C at ramping rate of 100 K per hour under flowing argon. Then, one of five different gases, N_2, Ar, 0.9% O_2 in Ar, air and 50% H_2O in air, was introduced into the reactor with the gas velocity of 3.5 m s^{-1} in a down-flow mode. After heat treatment, for a period of 4 h, the reactor was cooled to ambient temperature. The surfaces of the SiC coupons were analyzed by microRaman spectroscopy and SEM–EDX (FE-SEM Philips XL30) spectroscopy. Raman spectra were recorded at room temperature using a Renishaw inVia confocal microscope system with 514.5 nm excitation from an argon ion laser source at an incident power of 10 mW and with a spot size of 1.3 μm.

3. Results and discussion

The representative SEM images for the surface of pristine and heat-treated SiC coupons are present in Fig. 1. We have noticed that free carbon was left on the surface of pristine sample from the sintering process of manufacturing (Fig. 1a). After the treatment with argon, carbon has been found to be removed due to the oxidation by oxygen-containing impurities in argon. As a result, clear grain boundary is seen in Fig. 1b. Corresponding to this, the ratio of carbon to silicon from EDX decreases (Fig. 1b) in comparison to that from the pristine coupon. Under the experimental condition used in this study, the removal of carbon residues on the surface *via* oxidation seem to proceed under the diffusion controlled region, as considering the condition in the previous study [13]. Furthermore, the combination of the flat surface geometry of the SiC coupon and the gas velocity as high as 3.5 m s^{-1} in this study will significantly decrease the thickness of gas boundary layer on the surface, leading to the minimization of diffusion limitation for oxidants. Therefore, it is thought that oxidation rate of carbon residue is very rapid even under argon containing a trace of oxidizing impurity. Similarly, Pavese et al. reported that residual carbon from the pristine SiC surface was fully oxidized up to 1100 °C under air [14]. This supports that the free carbon, if any, from the pristine surface would be removed well below the temperature of 1400 °C, probably during the heating step in this study, before the silicon carbide surface is exposed to a gas selected for heat treatment.

Under oxygen and steam environments, provided that there is no concern on active oxidation of SiC, silicon carbide undergoes the surface oxidation through reactions (1) and (2) to form silicon oxide film. It is found that thick oxide film has formed on the coupon surface after being heat treated in 50% H_2O in air (Fig. 1c). Due to the thickness of oxide film on the SiC surface, the grain boundary was not observed in this case and the carbon peak in EDX has decreased significantly. Similar result was also found from the surface of SiC coupon treated under air (Fig. 1d). However, under the lower pressure of oxygen (i.e. 0.9% O_2 in argon), the heat treatment led to the formation of thinner oxide film on the SiC coupon. This resulted in the decrease in the ratio of oxygen to silicon peaks from the EDX in Fig. 1e. Due to the reduction in the thickness of oxide film, carbon peak associated with silicon carbide was also detected in the EDX in Fig. 1e. Formation rate of the oxide film in this study seems to be dependent on the partial pressure of oxidants, which is consistent with the literature [15].

$$\mathrm{SiC\ (s)+3/2O_2\ (g)\rightarrow SiO_2\ (s)+CO\ (g)},\quad \Delta G_{1400\,^\circ\mathrm{C}}=-813.4\ \mathrm{kJ/mol} \tag{1}$$

$$\mathrm{SiC\ (s)+3H_2O\ (g)\rightarrow SiO_2\ (s)+CO\ (g)+3H_2\ (g)},\quad \Delta G_{1400\,^\circ\mathrm{C}}=-349.4\ \mathrm{kJ/mol} \tag{2}$$

$$\mathrm{SiC\ (s)+SiO_2\ (s)+N_2\ (g)\rightarrow Si_2N_2O\ (s)+CO\ (g)},\quad \Delta G_{1400\,^\circ\mathrm{C}}=-62.7\ \mathrm{kJ/mol} \tag{3}$$

On being treated with nitrogen, the surface decomposition was found to have occured, leaving pits and holes on the coupon surface (Fig. 1f). From EDX, in addition to silicon and carbon atoms, nitrogen and oxygen were also detected. This may indicate that stable nitride film (Si_3N_4) has not formed on the surface. Gomez et al. [16] have reported that the conversion of SiC into Si_3N_4 during the nitridation required the temperature above 1450 °C and nitrogen pressure higher than 50 bar. At the present condition of atmospheric pressure of nitrogen, it seems that SiC with the native SiO_2 film reacts with nitrogen to produce silicon oxynitride (Si_2N_2O) through reaction (3), followed by decomposition into the gas phase species [17]. This is the possible reason for the decomposition of SiC surface in nitrogen environment in the present study.

Fig. 2 shows the Raman spectra obtained from the coupon-6s after being heat-treated in five different gases, together with one from a pristine SiC coupon. For the pristine sample, while there is no detectable peak in the acoustic mode region (Fig. 2a), the spectrum in the optical mode region between 1200 and 1800 cm^{-1} (Fig. 2b) is dominated by two carbon-induced peaks, the D peak from the defective structure and the G peak from the in-plane E_{2g} mode at ca. 1360 and 1590 cm^{-1}, respectively. In the absence of any peaks associated with SiC, these peaks reflect that the surface free carbon remained on the surface of pristine coupons. For the heat-treated coupons, the peaks assigned to 6H-SiC are observed at 150, 241 and 265 cm^{-1} in the frequency region of acoustic mode [10]. As observed in the similar condition [18], it is believed that α-cristobalite is produced as the protective layer after the treatment under oxidative environments in this study.

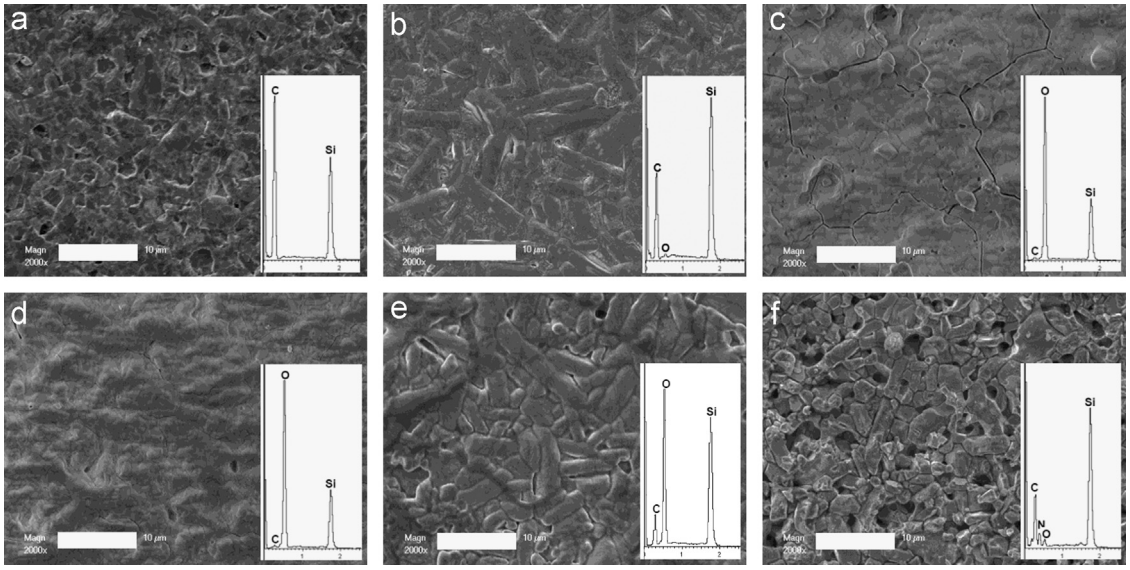

Fig. 1. SEM microphotographs with EDX spectroscopy (insets) of pristine 6H-SiC and those heat-treated under different atmospheres at 1400 °C [note: air and argon were used as balance for conditions described in (c) and (e), respectively. Scale bar = 10 μm].

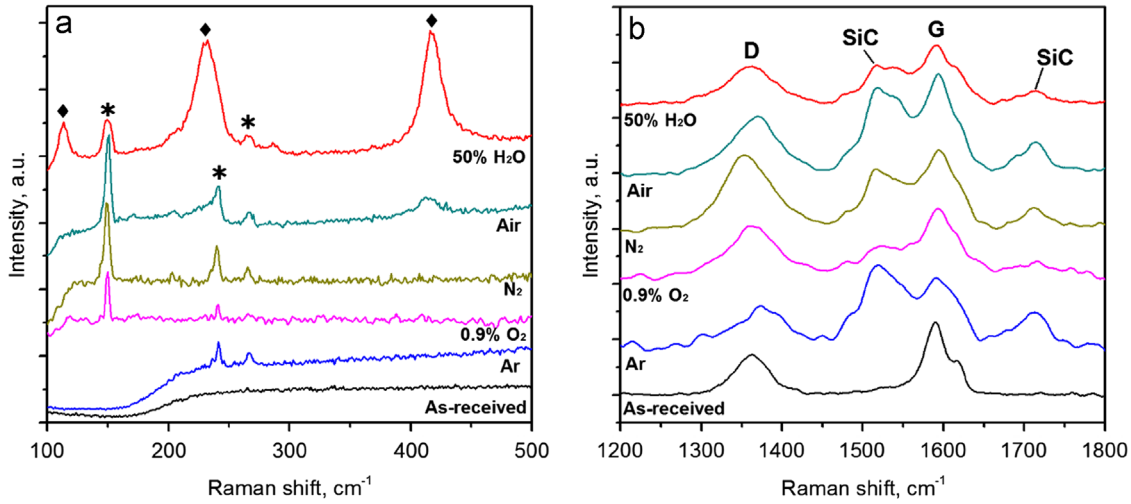

Fig. 2. Changes in Raman spectra in the frequency region of acoustic mode (a) and of optical mode (b) collected from 6H-SiC coupons after heat treatment in different atmospheres at 1400 °C [♦: Raman bands attributed to SiO_2, α-cristobalite; and ✱: Raman bands for 6H-SiC].

Raman-active peaks for α-cristobalite becomes prominent at 113, 231 and 417 cm^{-1} [19,20] for the coupons heat-treated using the higher oxygen partial pressure (i.e. 50% H_2O and air). For the coupon treated in 0.9% O_2 in argon, no peak associated with α-cristobalite is observed. This is probably because the oxide thickness on the surface is too thin, which might be below the detectable limit in the set parameters of Raman instrument. In Fig. 2b, except for the pristine sample, for all other heat-treated samples, the peaks originated from 6H-SiC appeared prominent at 1516 and 1714 cm^{-1} [21,22]. However, carbon-related D and G peaks are still observed for all samples after the heat treatment. The surface free carbon on pristine coupon is believed to have been oxidized even during the temperature ramp stage in argon atmosphere. Therefore, it is obvious that the carbon-related Raman peaks from the heat-treated samples are not attributed to the residual carbon on the surface. Then, the possible occasions for carbon formation should be considered. It was reported that the enrichment of C on the surface occurred through the graphitization of SiC during the heat treatment in the inert environment even at atmospheric pressure [23]. However, this possibility should be ruled out in this study. This is because the graphitization of SiC, which is accompanied by Si sublimation, requires a temperature higher than 1550 °C. Another possible occasion for the carbon production on the surface under oxygen environment is the reaction of SiC with oxygen, producing SiO_2 and C, as reported previously [24,25]. However, under the circumstance where Si and O are mainly detected from EDX in Fig. 1c–e, it is hard to believe that SiO_2 (s) and C (s) are produced together on the surface. Furthermore, even if any carbon is produced on the surface, it may readily undergo the oxidation process. Therefore, regardless of the type of gas used

in the treatment, carbon-related peaks in Raman spectra for those heat-treated in the present study should be considered to have originated from the place other than the top surface.

While direct carbon formation on the surface of SiC is unlikely to happen in this study, it should be pointed out that carbon containing structures such as graphitic layer can be formed in the SiO_2/SiC interface upon oxidation [26,27]. Chang et al. [26] observed the relative high C concentration at the SiO_2/SiC interface from electron energy loss spectroscopy (EELS) analysis. By means of the similar EELS analysis, Zheleva et al. [27] also found that C/Si ratio increased at the SiO_2/SiC interface. Although the clear understanding of the mechanism for the formation of interfacial carbon structure is still the subject of future studies, it is believed that oxygen diffusing through silica layer reacts with Si and residual C forms the graphitic structure or can be released as CO during oxidation of SiC [27,28]. Presumably, those carbon formed at the interface undergoes the structural change during the heat treatment. In order to determine the crystallinity of carbon structure, various parameters in Raman spectroscopy have been extensively used. It was reported that the G peak from graphitic carbon shifts to higher frequency with a decrease in the crystallinity, such as a reduction of the size of crystallites [29,30]. The intensity ratio of D to G peaks, $R(I_D/I_G)$, has been also widely used to investigate the structure of carbon materials [29,31]. Taking this into account, we deconvoluted the Raman spectra from Fig. 2b to evaluate carbon structure at the SiO_2/SiC interface. Then, the position of the G peak is plotted against $R(I_D/I_G)$ as shown in Fig. 3, where a linear trend is observed. Pristine sample shows the G peak position and $R(I_D/I_G)$ at 1589.4 cm^{-1} and 0.89, respectively. Starting from the point of the sample treated under 50% H_2O in air, the frequency of G peak and $R(I_D/I_G)$ combine to lead the trend towards the upper right-hand side, indicating a deterioration in the crystalline structure of the carbon. It is seen overall that the higher partial pressure of oxidizing component in the treatment gases is in favor of the formation of higher crystalline carbon structure at the interface. In other words, the shifting of G peak to higher frequency with higher value of $R(I_D/I_G)$ is intensified with the decrease in the partial pressure of oxidizing gas. It is believed that thick oxide film may kinetically limit the release of C atoms at the interface [26]. Thus, more C will be trapped at the interface during the heat treatment using the higher partial pressure of oxidizing gas, which produces thicker oxide film on the surface. This leads to the higher crystallinity in carbon structure produced at the SiO_2/SiC interface, suppressing the shifting of G peak to the higher frequency with higher value of $R(I_D/I_G)$. This explains how the trend in Fig. 3 is established.

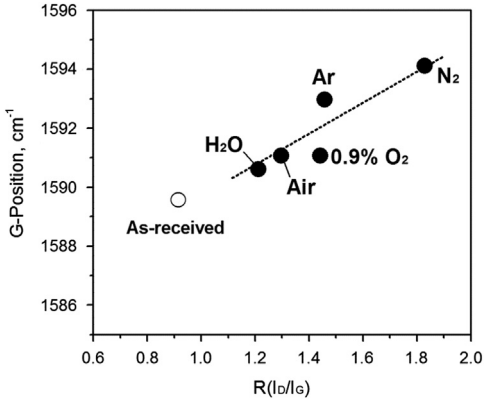

Fig. 3. Relationship between the position of G peak and $R(I_D/I_G)$ for the crystallinity of the produced graphitic carbon layer at the oxide film/SiC interface.

Raman spectroscopic analysis for SiC surface also allowed us to investigate the information on the surface defects in the present study. For the 6H-SiC polytype, characteristics of the Raman spectra are the folded transverse optical (FTO) and longitudinal optical (FLO) modes [10]. As seen in Fig. 4a and b, it is interesting to see the changes between the peaks in the FTO mode in this study. The peaks in FTO mode consist of three bands, which are assigned to the FTO(6/6), FTO(2/6) and FTO(0) bands. The FTO(6/6) and FTO(2/6) bands are located at 767 and 788 cm^{-1}, respectively. Another band, assigned to FTO(0), is observed at 797 cm^{-1}. This band is known to be sensitive to the stacking faults on the 6H-SiC [11]. As the representative results, Fig. 4a and b shows the Raman spectra from the SiC coupons-4 and -6 together with the curve-fitting results using the Lorentzian lines that were treated in 0.9% O_2 in argon at 1400 °C. As the intense FTO(2/6) bands are independent of stacking faults that exist on the surface of the SiC coupons [10,11], the intensity ratio of FTO(0) to FTO(2/6) bands are varied depending on the positions. The intensity ratio of the FTO(0) to FTO(2/6) bands for all SiC coupons, together with the temperature profile corresponding to the location of each SiC coupon in the reactor (Fig. 4c), is present in Fig. 4d. From the trend obtained, the lowest intensity ratio is recorded for coupon-6, at which the highest temperature was recorded in Fig. 4c. In overall, the intensity ratio of the FTO(0) to FTO(2/6) bands from the coupons followed the variation of temperature in the reactor. This may represent that the reduction in the density of stacking faults on the surface was maximized at the highest temperature region. We believe that the surface of the SiC coupons in the high temperature region undergoes a restructuring process, in which the degree of stacking disorder is reduced.

4. Conclusions

Effect of heat treatment under different gaseous environments on the surface of 6H-SiC coupons was investigated at 1400 °C. Heat treatment of SiC coupons under oxidative environments led to the formation of silicon oxide film, which was dependent on the partial pressure of oxidizing gas. Treatment with nitrogen resulted in the surface decomposition, where no detectable silicon nitride film was observed. It seems that SiC with the native SiO_2 film reacts with nitrogen to form silicon oxynitride, followed by decomposition into the gas phase species. Characterization of the heat treated SiC coupons by Raman spectroscopy and SEM–EDX revealed that the graphitic carbon layers were produced at SiO_2/SiC interfaces during heat treatment. A relationship between the position of the G peak and $R(I_D/I_G)$ was established for the order of crystallinity in the interfacial carbon structures. Crystallinity of

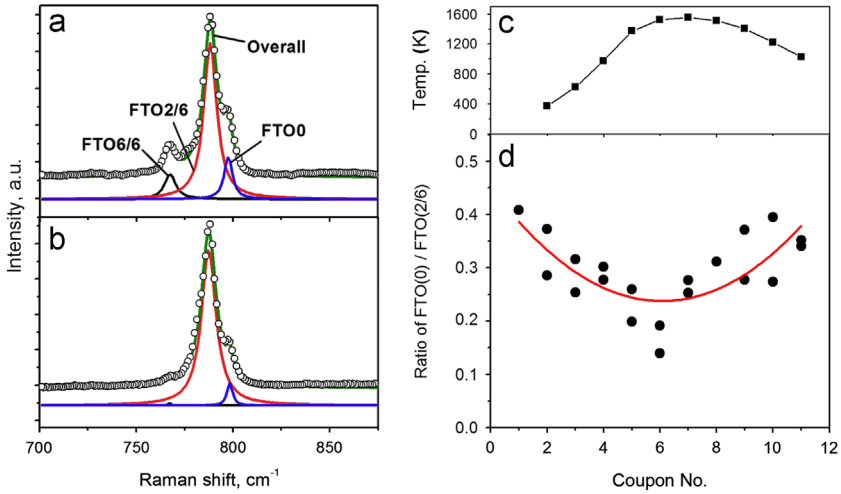

Fig. 4. Curve-fittings of Raman spectra collected from the coupon-4 (a) and -6 (b) after being exposed to 0.9% O_2 in Ar at 1400 °C (original spectra denoted in open circles). Temperature profile along the reactor (c) and the intensity ratio of the FTO(0)/FTO(2/6) bands in the Raman spectra collected from the surface of the SiC coupons heat-treated in 0.9% O_2 in Ar at 1400 °C (d).

carbon layer at the interface seemed to be dependent on the partial pressure of oxidizing gas, where more carbon tended to be trapped at the interface at higher partial pressure of oxidizing gas. Less crystalline carbon structure was formed from the treatment under inert environments such as argon and nitrogen that contained a trace amount of oxidizing sources. Furthermore, heat treatment under 0.9% oxygen in argon was found to have reduced the content of stacking faults on SiC surface. This was verified by the fact that the relative intensity of FTO(0) to FTO(2/6) bands gradually decreased with increasing the temperature in the reactor.

Acknowledgments

The support of this work by the Chevron Energy Technology Company is gratefully acknowledged. The authors thank Dr. Tracey Markley (CSIRO Materials Science and Engineering) for assistance with the Raman analysis.

References

[1] G.L. Harris, Properties of Silicon Carbide, INSPEC, Institution of Electrical Engineers, London, 1995.
[2] H.J. Sanders, High-tech ceramics, Chemical and Engineering News 62 (1984) 26–40.
[3] S. Tacchino, L.D. Vella, S. Specchia, Catalytic combustion of CH_4 and H_2 into micro-monolith, Catalysis Today 157 (2010) 440–445.
[4] Christian, M. Mitchell, D.P. Kim, P.J.A. Kenis, Ceramic microreactors for on-site hydrogen production, Journal of Catalysis 241 (2006) 235–242.
[5] A. Worner, R. Tamme, CO_2 reforming of methane in a solar driven volumetric receiver-reactor, Catalysis Today 46 (1998) 165–174.
[6] E. Klemm, H. Doring, A. Geisselmann, S. Schirrmeister, Microstructured reactors in heterogeneous catalysis, Chemical Engineering and Technology 30 (2007) 1615–1621.
[7] P.L. Mills, D.J. Quiram, J.F. Ryley, Microreactor technology and process miniaturization for catalytic reactions—a perspective on recent developments and emerging technologies, Chemical Engineering Science 62 (2007) 6992–7010.
[8] A. Renken, L. Kiwi-Minsker, Microstructured catalytic reactors, Advances in Catalysis 53 (2010) 47–122.
[9] W.J. Lee, C. Li, N. Burke, D. Trimm, J. Patel, The growth and morphology of core/shell heterostructured conical carbon fibers, Carbon 49 (2011) 2735–2741.
[10] S. Nakashima, H. Harima, Raman investigation of SiC polytypes, Physica Status Solidi A 162 (1997) 39–64.
[11] S. Nakashima, Y. Nakatake, H. Harima, M. Katsuno, N. Ohtani, Detection of stacking faults in 6H-SiC by Raman scattering, Applied Physics Letters 77 (2000) 3612–3614.
[12] Y. Ma, S. Wang, Z.H. Chen, Raman spectroscopy studies of the high-temperature evolution of the free carbon phase in polycarbosilane derived SiC ceramics, Ceramics International 36 (2010) 2455–2459.
[13] E.J. Opila, J.L. Serra, Oxidation of carbon fiber-reinforced silicon carbide matrix composites at reduced oxygen partial pressures, Journal of the American Ceramic Society 94 (2011) 2185–2192.
[14] M. Pavese, P. Fino, A. Ortona, C. Badini, Potential of SiC multilayer ceramics for high temperature applications in oxidising environment, Ceramics International 34 (2008) 197–203.
[15] N.S. Jacobson, Corrosion of silicon-based ceramics in combustion environments, Journal of the American Ceramic Society 76 (1993) 3–28.
[16] E. Gomez, T. Gomezacebo, J. Echeberria, I. Iturriza, F. Castro, Nitridation of SiC for the production of SiC–Si_3N_4 nanocomposites, Journal of the European Ceramic Society 14 (1994) 411–418.
[17] T.C. Ehlert, T.P. Dean, M. Billy, J.C. Labbe, Thermal-decomposition of the oxynitride of silicon, Journal of the American Ceramic Society 63 (3–4) (1980) 235–236.
[18] M. Maeda, K. Nakamura, T. Ohkubo, T. Ishizuka, Oxidation behavior of silicon carbide under cyclic and static conditions, Ceramics International 15 (1989) 1–6.
[19] I.P. Swainson, M.T. Dove, D.C. Palmer, Infrared and Raman spectroscopy studies of the alpha–beta phase transition in cristobalite, Physics and Chemistry of Minerals 30 (2003) 353–365.
[20] J.B. Bates, Raman spectra of alpha-cristobalite and beta-cristobalite, Journal of Chemical Physics 57 (1972) 4042–4047.
[21] J.C. Burton, L. Sun, F.H. Long, Z.C. Feng, I.T. Ferguson, First- and second-order Raman scattering from semi-insulating 4H-SiC, Physical Review B 59 (1999) 7282–7284.
[22] H.W. Kunert, T. Maurice, J. Barnas, J. Malherbe, D.J. Brink, L. Prinsloo, Raman and photoluminescence spectroscopy from n- and p-type 6H-SiC alpha-particle irradiated, Vacuum 78 (2005) 503–508.
[23] K.V. Emtsev, A. Bostwick, K. Horn, J. Jobst, G.L. Kellogg, L. Ley, J. L. McChesney, T. Ohta, S.A. Reshanov, J. Rohrl, E. Rotenberg, A. K. Schmid, D. Waldmann, H.B. Weber, T. Seyller, Towards wafer-size

graphene layers by atmospheric pressure graphitization of silicon carbide, Nature Materials 8 (2009) 203–207.
[24] K. Negita, Effective sintering aids for silicon carbide ceramics: reactivities of silicon carbide with various additives, Journal of the American Ceramic Society 69 (1986) C308–C310.
[25] Z.H. Yang, D.C. Jia, Y. Zhou, P.Y. Shi, C.B. Song, L. Lin, Oxidation resistance of hot-pressed SiC–BN composites, Ceramics International 34 (2) (2008) 317–321.
[26] K.C. Chang, N.T. Nuhfer, L.M. Porter, Q. Wahab, High-carbon concentrations at the silicon dioxide–silicon carbide interface identified by electron energy loss spectroscopy, Applied Physics Letters 77 (2000) 2186–2188.
[27] T. Zheleva, A. Lelis, G. Duscher, F. Liu, I. Levin, M. Das, Transition layers at the SiO_2/SiC interface, Applied Physics Letters 93 (2008) 022108.
[28] M. Di Ventra, S.T. Pantelides, Atomic-scale mechanisms of oxygen precipitation and thin-film oxidation of SiC, Physical Review Letters 83 (1999) 1624–1627.
[29] A. Cuesta, P. Dhamelincourt, J. Laureyns, A. Martinezalonso, J.M. D. Tascon, Raman microprobe studies on carbon materials, Carbon 32 (1994) 1523–1532.
[30] G. Irmer, A. Dorner-Reisel, Micro-Raman studies on DLC coatings, Advanced Engineering Materials 7 (2005) 694–705.
[31] A.C. Ferrari, J. Robertson, Interpretation of Raman spectra of disordered and amorphous carbon, Physical Review B 61 (2000) 14095–14107.